Electronic Supplementary Material (ESI) for RSC Advances.

Electronic Supporting Information

Mechanistic investigations of bifunctional squaramide organocatalyst in asymmetric Michael reaction, observation of stereoselective retro-Michael reaction

*Eszter Varga, László Tamás Mika, Antal Csámpai, Tamás Holczbauer, György Kardos and Tibor Soós**

I. Characterization of catalyst 3

A. Characterization of catalyst 3 by NMR spectroscopy

*The preparation of 3-(benzylamino)-4-(((1S)-(6-methoxyquinolin-4-yl)((2S,4S,5R)-5-vinylquinuclidin-2-yl)methyl)amino)cyclobut-3-ene-1,2-dione (catalyst **3**)*

To the solution of diethyl squarate (10.0 mmol, 1.702 g) in diethyl ether (10 ml) benzylamine (11.0 mmol, 1.179 g) was added drop wise over a period of 5 minutes at ambient temperature and stirred overnight. A small amount of white powder precipitated which was removed by filtration. 9-amino(9-deoxy)epihydroquinine (11 mmol) was added to the filtrate and stirred overnight at room temperature. The catalyst precipitated and was separated by filtration and washed with diethyl ether (2x 10 ml) to yield 4.424 g (87 % yield).
Nuclear Magnetic Resonance spectra (NMR) were acquired on a Bruker DRX-500 (500 MHz) instrument using TMS as internal standard. All assignments of the catalyst **3** are confirmed by 2D-COSY, 2D-HSQC, 2D-HMBC and NOESY measurements.
The structure of the catalyst **3** was determined in $CDCl_3$ solution by ^{1}H- and ^{13}C NMR measurements at 310 and 320 K, respectively. Assignments were confirmed by 2D-COSY, 2D-HSQC, 2D-HMBC and NOESY methods.

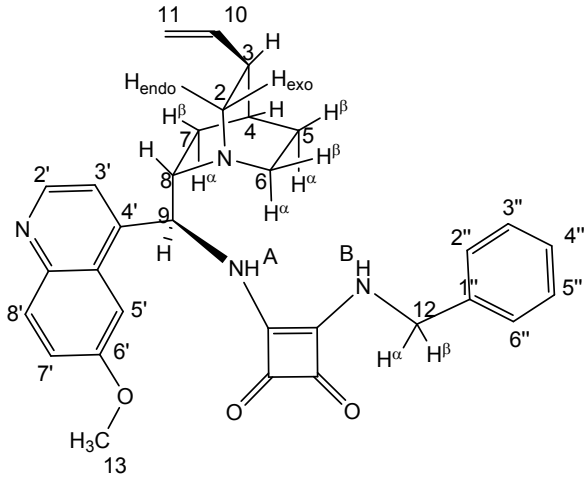

^{1}H-NMR (500 MHz, $CDCl_3$, T = 300?): δ ppm 8.61 (d, *J*=4.4 Hz, 1H, H-2'), 8.01 (d, *J*=9.2 Hz, 1H, H-8'), 7.77 (br s, 1H, H-5'), 7.48 (br s, 1H, H-3'), 7.40 (dd, *J*=2.5, 9.2 Hz, 1H, H-7'), 7.11 (br m 3H, Ph-3"4"5"), 6.92 (br d, *J*=4.7 Hz, 2H, Ph-2"6"), 6.07 (br s, 1H, H-9), 5.78 (td, 1H, H-10), 5.01 (d, *J*=17.2 Hz, 1H, H^α-11), 4.96 (d, *J*=10.4 Hz, 1H, H^β-11), 4.35 (dd, *J*=14.3, 61.2 Hz, 2H, $H^{\alpha\beta}$-12), 3.92 (s, 3H, H-13, -OCH_3), 3.52 (br s, 1H, H-8), 3.40 (s, 1H, H^α-6), 3.20 (dd, *J*=10.4, 13.5 Hz, 1H, H^{exo}-2), 2.79 (br d, *J*=13.4 Hz, 1H, H^{endo}-2), 2.72 (m, 1H, H^β-6), 2.29 (br s, 1H, H-3), 1.66 (br s, 1H, H-4), 1.59 (br s, 2H, H-5$^{\alpha\beta}$), 1.45 (t, *J*=11.0 Hz, 1H, H^β-7), 0.75 (s, 1H, H^α-7). ^{13}C-NMR (500 MHz, $CDCl_3$, T = 310? K) δ ppm 167.5 (C-14), 159.2 (C-6'), 148.3 (C-4'), 147.5 (C-2'), 144.6 (C-8'a), 141.5 (C-10), 138 (C-1''), 130.6 (C-8'), 129.4 (C-4a'), 128 (C-2''), 122.3 (C-7'), 120.2 (C-3'), 115.2 (C-11), 102.1 (C-5'), 60.2 (C-8), 56.4 (C-13), 56.3 (C-2), 53.3 (C-9), 48.1 (C-12), 41 (C-6), 39.6 (C-3), 27.9 (C-4), 27.9 (C-5), 25.9 (C-7)

The effect of temperature to the conformation was investigated. Based on the comparison of the ^{1}H-NMR spectra of catalyst **3** at two different temperatures, it can be seen that the molecule can freely rotate around the C8-C9 bond and the quinuclidine and quinoline ring is sensitive to this conformation changes.

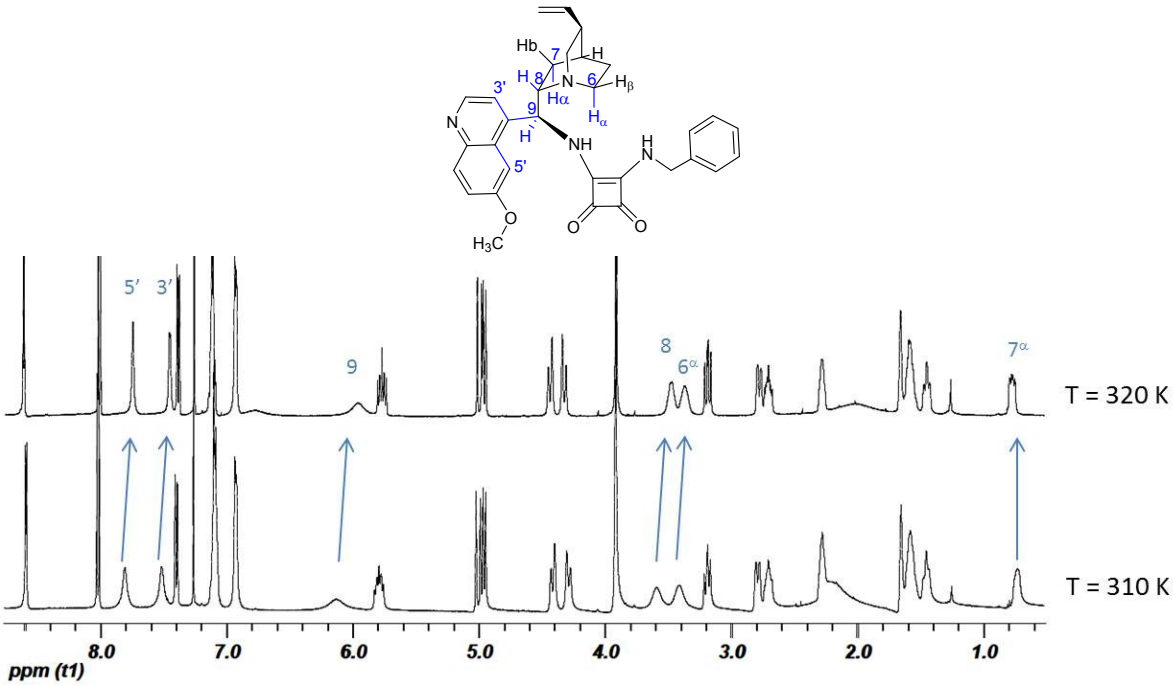

Figure 1. ^{1}H spectra of catalyst **3** at different temperatures.

The chemical shifts of ^{13}C NMR signals were obtained and assigned in the 2D spectra on the basis of the cross-peaks discernible.

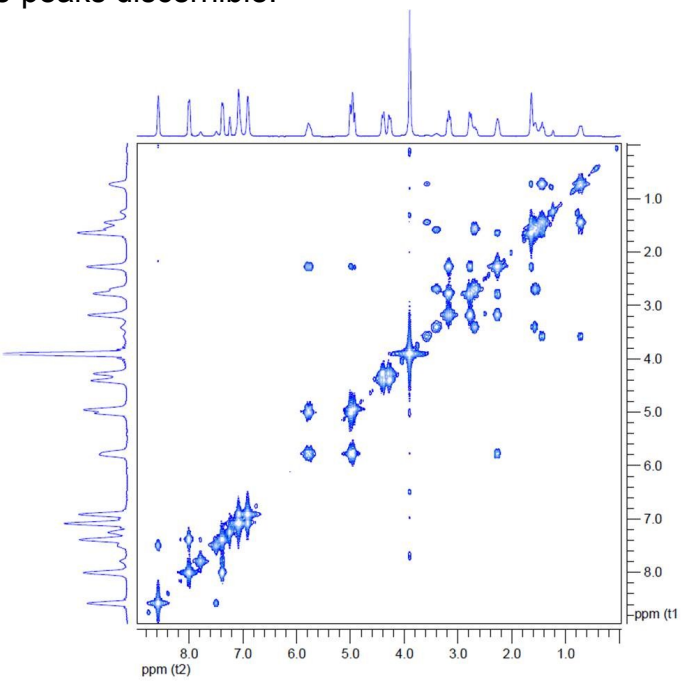

Figure 2. COSY spectra of catalyst **3** in $CDCl_3$.

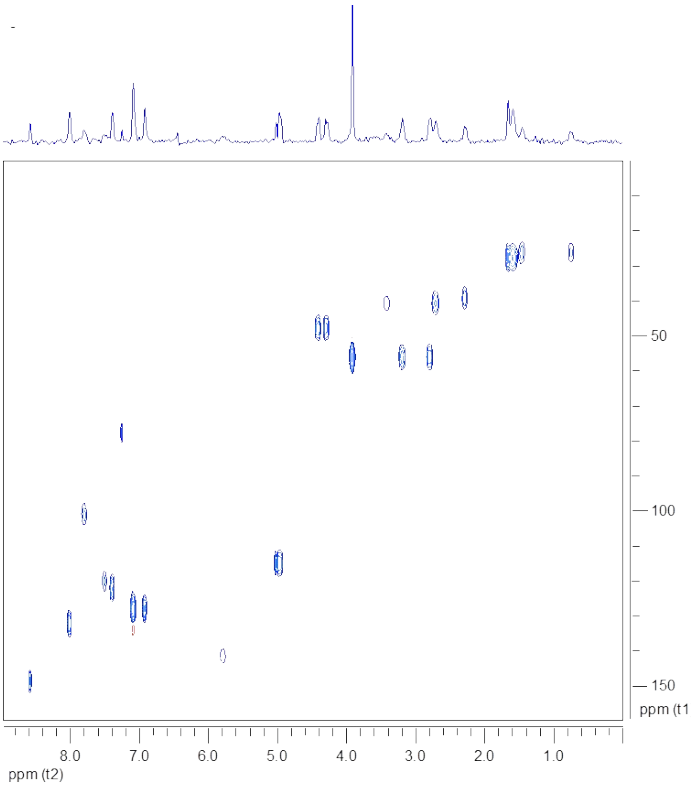

Figure 3. HSQC spectra of catalyst **3** in $CDCl_3$.

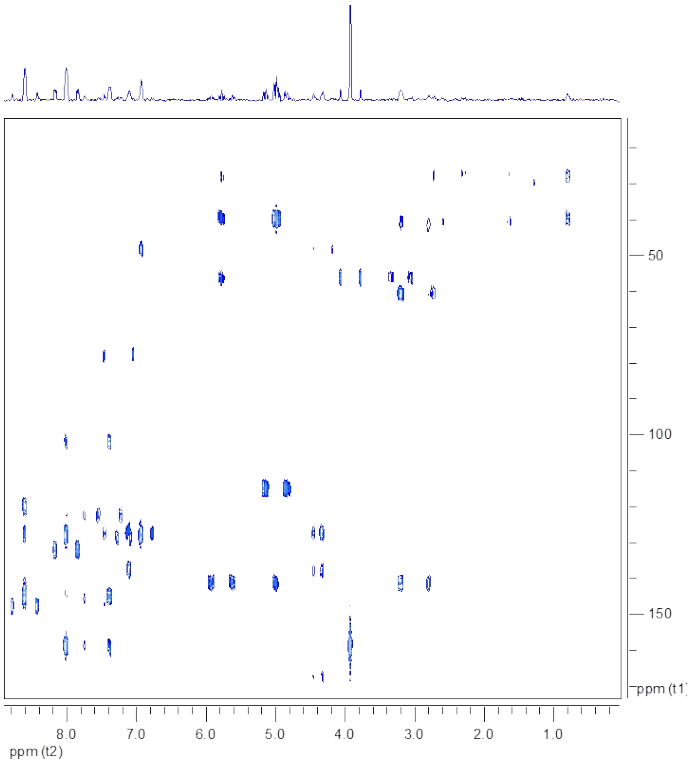

Figure 4. HMBC spectra of catalyst **3** in $CDCl_3$.

B. Characterization of catalyst 3 by X-Ray study

Additionally, the solid state structure of the catalyst **3** was determined by X-ray diffraction. The X-ray crystal structure is in consistence with the structures in solution determined by NMR spectroscopy. On the other hand, it is not sure that the conformer in solid phase determined by molecular packing fully corresponds to that adopted in solution relevant to catalytic activity.

X-ray crystallographic data were collected on a Rigaku R-AXIS-RAPID diffractometer[1] (graphite monochromator). Crystallographic data (excluding structure factors) for the structure in this paper have been deposited with the Cambridge Crystallographic Data Centre as supplementary publication CCDC no. **1412465**. Copies of the data can be obtained, free of charge, on application to CCDC, 12 Union Road, Cambridge CB2 1EZ, UK, (fax: ţ44-(0)1223 336033 or e-mail: deposit@ccdc.cam.ac.uk).

Crystal data: $C_{31}H_{32}N_4O_3$, *Fwt.*: 508.60, colourless, platelet, size: 0.25 x 0.25 x 0.05 mm, orthorhombic, space group $P2_12_12_1$, a = 8.7790(2)Å, b = 11.6400(2)Å, c = 26.194(1)Å, α = 90°, β = 90°, γ = 90°, V = 2676.7(1)Å^3, T = 295(2)K, Z= 4, F(000) = 1080, D_x = 1.262 Mg/m^3, μ 0.659mm^{-1}.
A crystal of SHELX was mounted on a loop. Cell parameters were determined by least-squares using 21339 ($6.50 \leq \theta \leq 71.50°$) reflections.
Intensity data were collected on a RAXIS-RAPID diffractometer (monochromator; Cu-$K\alpha$ radiation, λ = 1.54178Å) at 295(2) K in the range $6.538 \leq \theta \leq 56.906$[2]. A total of 23228 reflections were collected of which 3579 were unique [R(int) = 0.0293, $R(\sigma)$ = 0.0304]; intensities of 2886 reflections were greater than $2\sigma(I)$. Completeness to θ = 0.995.
A numerical absorption correction[3] was applied to the data (the minimum and maximum transmission factors were 0.826 and 0.941).
The structure was solved by direct methods[4] (and subsequent difference syntheses).
Anisotropic full-matrix least-squares refinement[4] on F^2 for all non-hydrogen atoms yielded R_1 = 0.0333 and wR^2 = 0.0657 for 1332 [$I>2\sigma(I)$] and R_1 = 0.0547 and wR^2 = 0.0900 for all (3579) intensity data, (number of parameters = 345, goodness-of-fit = 1.192, the maximum and mean shift/esd is 0.000 and 0.000). The absolute structure parameter is 0.01(5). (Friedel coverage: 0.723, Friedel fraction max.: 0.990, Friedel fraction full: 0.990).
The maximum and minimum residual electron density in the final difference map was 0.18 and -0.19 e.Å^{-3}.
The weighting scheme applied was $w = 1/[\sigma^2(F_o^2)+(0.02400.9144P)^2+0.9144P]$ where $P = (F_o^2+2F_c^2)/3$.
Hydrogen atomic positions were calculated from assumed geometries except H1A, H1B that were located in difference maps. Hydrogen atoms were included in structure factor calculations but they were not refined. The isotropic displacement parameters of the hydrogen atoms were approximated from the U(eq) value of the atom they were bonded to.

---

[1] A diffractometer purchase grant from the National Office for Research and Technology (MU-00338/2003) is gratefully acknowledgement.

[2] CrystalClear SM 1.4.0 (Rigaku/MSC Inc., 2008).

[3] NUMABS: Higashi, T. (1998), rev. 2002. (Rigaku/MSC Inc.)

[4] G.M. Sheldrick, *Acta Cryst.* (2008). **A64**, 112-122.

ORTEP style molecular structure diagram can be found in Figure 5, while crystallographic data are in Table 1.[5]

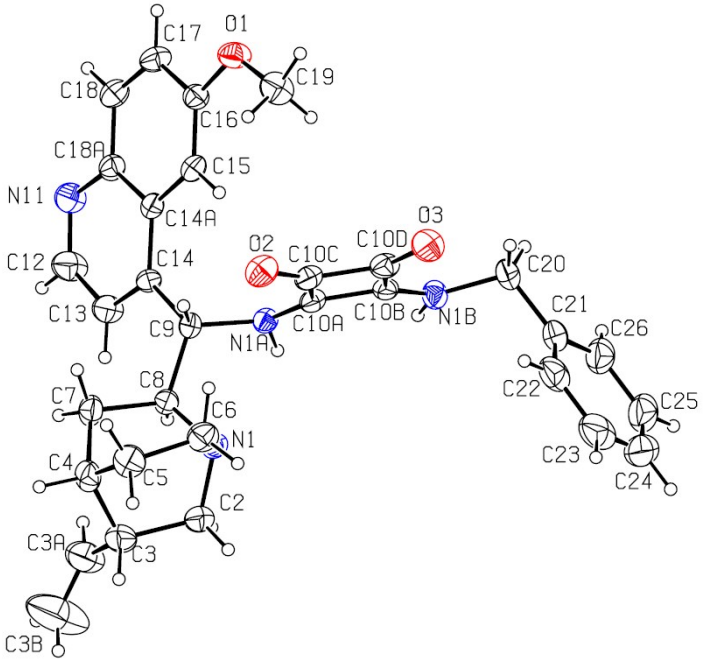

Figure 5. The crystallographically independent molecule in the asymmetric unit of the crystal **3** with the atomic labelling. Displacement ellipsoids are drawn at the 30% probability level.

[5] PLATON: Spek, A.L. *J.Appl.Cryst.* (2003), **36**, 7-13.

Table 1. Crystal data and structure refinement

Empirical formula	$C_{31}H_{32}N_4O_3$
Formula weight	508.60
Temperature	295(2)
Radiation and wavelength (Å)	Cu-Kα, λ =1.54178
Crystal system	orthorhombic
Space group	*P* 21 21 21
Unit cell dimensions	
a (Å)	8.7790(2)
b (Å)	11.6400(2)
c (Å)	26.194(1)
α (°)	90°
β (°)	90°
γ □°□	90
Volume (Å^3)	2676.7(1)
Z	4
Density (calculated) (Mg/m^3)	1.262
Absorption coefficient, μ (mm^{-1})	0.659
F(000)	1080
Crystal colour, description	colourless, platelet
Crystal size (mm)	0.25 x 0.25 x 0.05
Absorption correction	numerical
Max. and min. transmission	0.826 and 0.941
θ□range for data collection (°)	6.538 ≤ θ ≤ 56.906
Index ranges	-9 ≤ □ ≤9; -12≤□□ ≤12; -27 ≤ □□≤ 28
Reflections collected	23228
Completeness to 2θ	0.995
Absolute structure parameter	
Flack (*x*)	0.01(5)
Hooft (*y*)	0.01(8)
Parsons (*z*)[6]	-0.01(8)
Friedel coverage	0.723
Friedel fraction max.	0.990
Friedel fraction full	0.990
Independent reflections	3579 [*R*(int) =0.0293]
Reflections *I*>2σ(*I*)	2886
Refinement method	full-matrix least-squares on F^2
Data / restraints / parameters	3579 /0 /345
Goodness-of-fit on *F*2	1.192
Final *R* indices [*I*>2σ(*I*)]	R_1 =0.0333, wR^2 =0.0657
R indices (all data)	R_1 =0.0547, wR^2 =0.0900
Max. and mean shift/esd	0.000;0.000
Largest diff. peak and hole	0.18 and -0.19 e.Å^{-3}

[6] S. Parsons, H. Flack, *Acta Cryst*. (2004), A60, s61.

*Comparison of crystal structure of molecule **3** and other quinine-squaramide structures from the literature*

The molecule **3** stands by the hydrogen bond acceptor isoquinoline and quinuclidine groups, and by the hydrogen bond donor squaramide groups. The aromatic attribution of the phenyl groups and isoquinoline groups are important organiser forces in the crystal lattices as well.
Two similar conformation squaramide crystal structures were found in the literature with similar isoquinoline, quinuclidine and phenyl groups[7],[8]. One of them (**UBADUY**)[7] has the same *R, S, S, S* configuration, the case of **NOLRIQ**[8] the atoms have *R, S, R, R* configuration.
In the crystal lattices of **NOLRIQ** and **3** there are hydrogen bonds interactions between the squaramides moieties of the neighbour molecules. These interactions are the strongest secondary interaction in the lattices because of the high acidity of squaramide. In consequence these contacts are the prime organiser forces in the crystal lattice[9]. In the **NOLRIQ** there are additional π···F and H···F secondary interactions (Figure 6.).

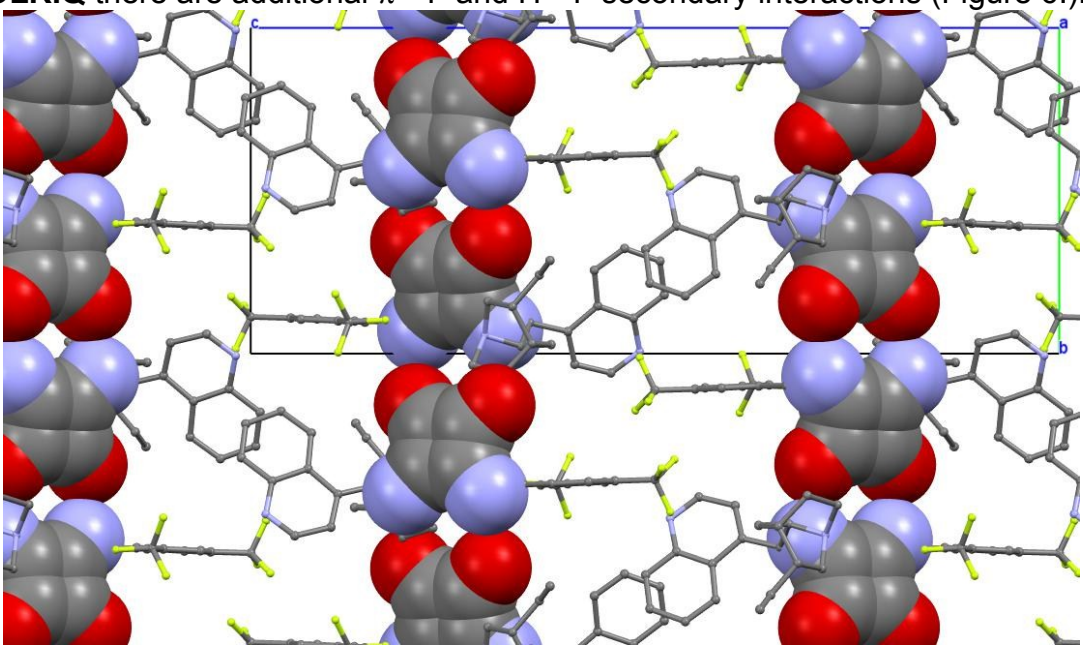

Figure 6. The layers of molecules (NOLRIQ) connected by strong squaramides···squaramides hydrogen bonds secondary interaction and an other aromatic layer can be observed in the crystal lattice (showed by using program Mercury10).

In the **UBADUY** structure a water molecule is connected with N-H···O type hydrogen bonds to the squaramides.
Molecule **3**, **NOLRIQ** and **UBADUY** molecules have similar conformation (Figure 7.), only the placement of the phenyl rings and isoquinoline rings differ. The phenyl ring turned at the CH_2 atoms by 87(2)°, the isoquinoline group turned by 43(3)°.

[7] L. Dai, H. Yang, F. Chen, *Eur. J. Org. Chem.*, **2011**, 5071–5076
[8] J. P. Malerich, K. Hagihara, V. H. Rawal, *J. Am. Chem. Soc.*, **2008**, 130, 14416–14417
[9] R. I. Storer, C. Aciro, L. H. Jones, *Chem. Soc. Rev.*, **2011**,40, 2330–346
[10] C. F. Macrae, I. J. Bruno, J. A. Chisholm, P. R. Edgington, P. McCabe, E. Pidcock, L. Rodriguez-Monge, R. Taylor, J. van de Streek, P. A. Wood, *J. Appl. Cryst.*, **2008**, 41, 466-470

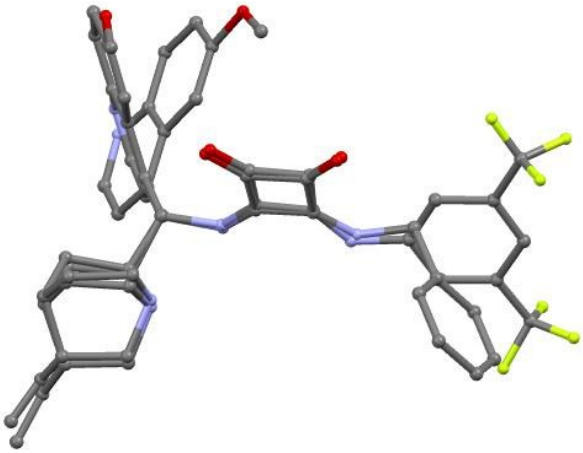

Figure 7. Molecular overlay of structure **3** and UBADUY to observe conformation differences[10].

UBADUY structure lattice enclathrates a toluene molecule (Figure 8.). Its placement is enclosed by π···π and CH···π interactions.

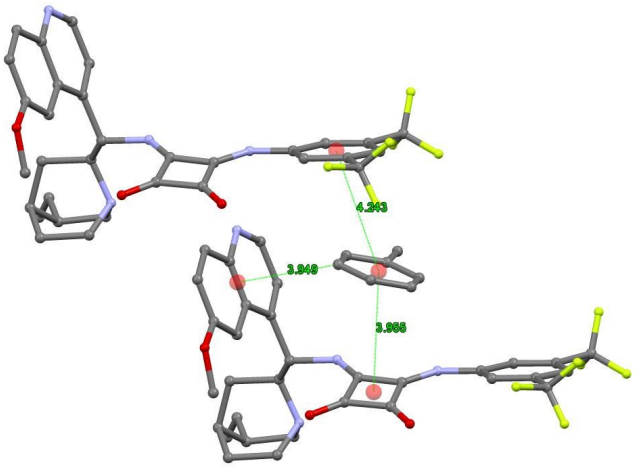

Figure 8. The aromatic interactions of the enclosed toluene in the UBADUY crystal lattice.

In absence of the enclathrated solvent the toluene, the phenyl groups turn to the neighbouring isoquinoline groups as it happens in the case of structure of **3**. (Figure 9.).

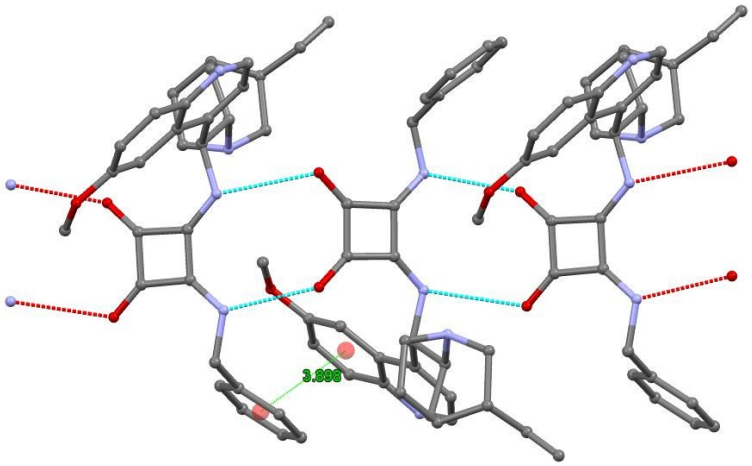

Figure 9. In the measured crystal **3** the molecules form a layer of alternating molecules connected by the squaramides···squaramides hydrogen bonds, strengthened by π ···π interaction as well.

II. Detailed results of kinetic studies

A. Calibration of IR measurements

The starting materials and the product were dissolved in $CHCl_3$ and measured separately by FTIR and a calibration set was carried out. In all case the most intensive and non-overlapping bands were selected and the calibration factor were determined based on Lambert-Beer's law (A= ε*c*l). The following bands were selected: Acetylacetone (**2**): 1621 cm^{-1} (ν C=O); β-Nitrostyrene (**1**): 1345 cm^{-1} (ν NO_2); 3-(2-nitro-1-phenylethyl)-pentane-2,4-dione (**4**): 1556 cm-1 (ν NO_2)

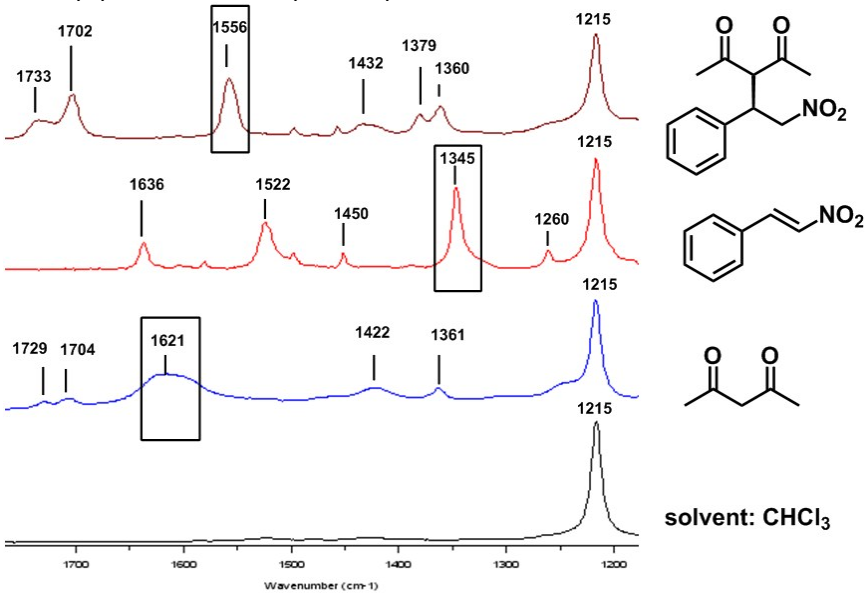

Figure 10. The recorded IR spectra of the 1 M solution of the reactants and the solvent.

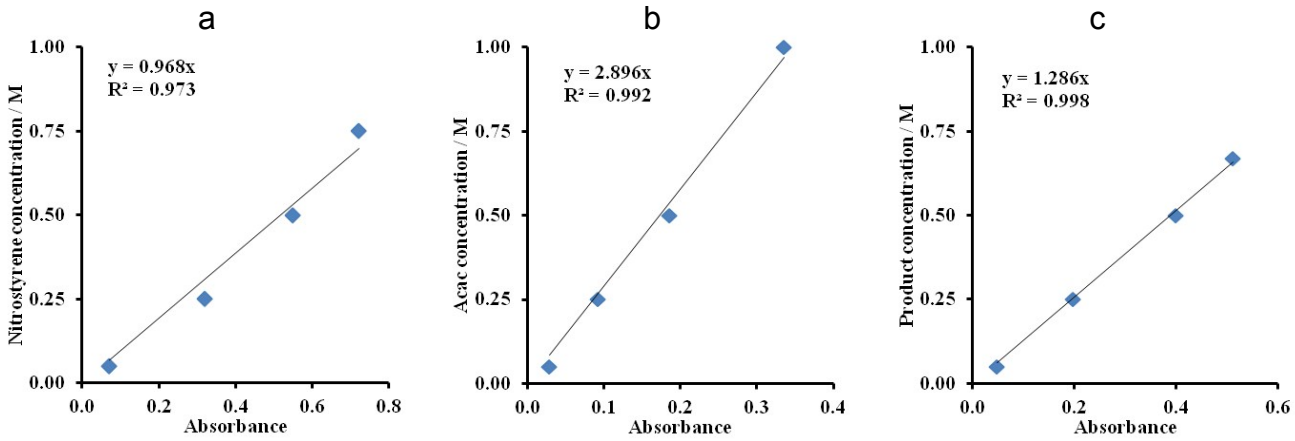

Figure 11. Calibration curves of FTIR absorbance: a) Absorbance of β-nitrostyrene (**1**) (c = 0.05-0.75 M), b) Absorbance of acetylacetone (**2**) (c = 0.05-1.0 M) c) Absorbance of the Michael adduct (**4**) (c = 0.05-0.75 M)

β-Nitrostyrene (**1**): (ε*l) = **0.968**, at 1345 cm^{-1} (ν NO_2)
Acetylacetone (**2**): (ε*l) = **2.896**, at 1621 cm^{-1} (ν C=O)
Product (**4**): 3-(2-nitro-1-phenylethyl)-pentane-2,4-dione: (ε*l) = **1.286**, at 1556 cm^{-1} (ν NO_2)

B. General procedure for *in situ* IR experiments

Infrared spectra were recorded with a ReactIR 1000 Reaction Analysis System attached to atmospheric pressure silicon (SiComp™) probe head. *In situ* IR experiments were performed in a three necked 25 ml glass flask. In every 2 minutes 64 scan were recorded between 4000-600 cm^{-1}, with resolution of 4 cm^{-1} and the mean was converted to a single spectrum. The reaction was stopped after 1-3 h depending on the conversion. In some cases the spectra were recorded in every 1 minute registering 32 scans. From the selected bands were generated a quick profile of the reaction (Figure 12.) and the concentrations were calculated based on calibration.

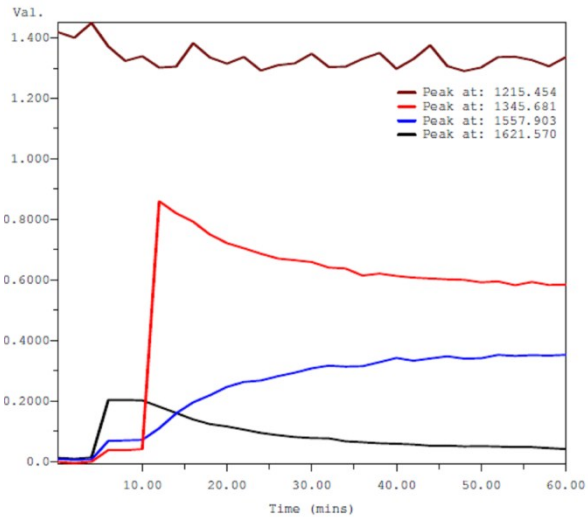

Figure 12. Quick profile of a representative reaction using ReactIR 1000.

C. Method of reaction rate calculation

The reaction rate was generated from the concentration versus time plot by mathematically differentiating the fifth–order best fit polynomial f(*t*). (Since this is empirical method, df(*t*)/dt is valid only over the range of reactants for which experimental data was collected) There are three representative plot on Figure 13.

To test the reproducibility of the measurement, three parallel measurements were carried out at same conditions. The deviation of calculated initial rate was 18 %, and this value was applied for further calculations.

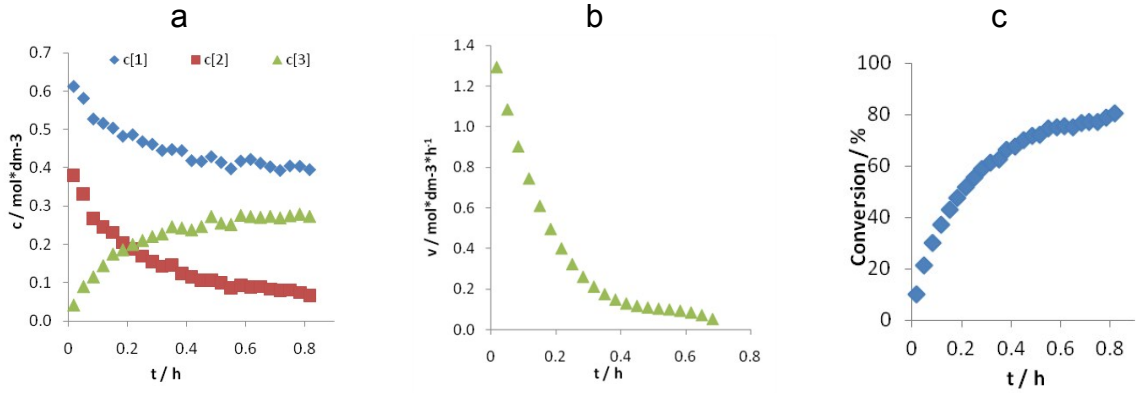

Figure 13. a) Reactant concentrations during the reaction, $[1]_0$ =0.6 M, $[2]_0$ = 0.3 M, [3] = 0.006 M; b) Reaction rate vs. time plot by the same reaction, c) Conversion vs. time plot by the same reaction

D. Calculation of observed rate constant

The rate equation of this reaction could be written in the form:
$v = k \cdot [\mathbf{1}]^n \cdot [\mathbf{2}]^m \cdot [\mathbf{3}]^o \cdot [\mathbf{4}]^p$

Determination the order of the catalyst (**3**):
By measuring the reaction rate at different catalyst loadings (from 0.003 to 0.021 M), it was determined that the reaction is first-order in catalyst **3**. The data according to Fig. 3 in the article is presented on Table 2.

Table 2. Reaction conditions and reaction rate using different catalyst (**3**) concentration

Nr.	Catalyst loading / mol%	[3] / M	v_0 / M*h^{-1}	ln $[1]_0$	ln v_0
A: $[1]_0$ = 0.3 M, $[2]_0$ = 0.6 M					
1	1	0.0030	0.351	-5.809	-1.047
2	1.5	0.0045	0.569	-5.404	-0.564
3	2	0.0060	1.205	-5.116	0.186
4	4	0.0120	1.944	-4.423	0.665
5	5	0.0150	2.962	-4.200	1.086
6	6	0.0180	3.466	-4.017	1.243
7	7	0.0210	4.280	-3.863	1.454
B: $[1]_0$ = 0.6 M, $[2]_0$ = 0.3 M					
8	1	0.0030	0.308	-5.809	-1.179
9	1.5	0.0045	1.004	-5.404	0.004
10	2	0.0060	1.474	-5.116	0.388
11	4	0.0120	2.847	-4.423	1.046
12	5	0.0150	3.055	-4.200	1.117
13	6	0.0180	3.782	-4.017	1.330
14	7	0.0210	5.007	-3.863	1.611

The order of the reactants was determined by changing the initial concentration of the given substrate, while the other parameters were kept constant. Accordingly, the rate equation could be further simplified. The apparent rate constant was calculated based on logarithmic transformation.

The order of the nucleophile (**2**) was determined in the non-saturated regime I. and the reaction rate dependence was found less than first-order in nucleophile concentration. The data according to Fig. 5 in the article is presented on Table 3.
The order of the nucleophile (**2**) was determined based on following equations:
$v = k_{obs}*[2]^m$
$\ln v = m*\ln[2] + \ln k_{obs}$

Table 3.: Reaction conditions and reaction rate using different acetylacetone concentration

	Nr.	$[2]_0$ / M	v_0 / M*h^{-1}	$\ln [2]_0$	$\ln v_0$
$[1]_0$ = 0.3 M, catalyst: [3] = 0.006 M					
Non-saturated regime I	1	0.15	0.267	-1.897	-1.321
	2	0.30	0.500	-1.204	-0.693
	3	0.38	0.664	-0.981	-0.409
	4	0.60	0.860	-0.511	-0.151
	5	0.75	1.171	-0.288	0.158
Regime II.	6	0.90	1.189		
	7	1.50	1.106		
$[1]_0$ = 0.6 M, catalyst: [3] = 0.006 M					
Non-saturated regime I	8	0.15	1.010	-1.897	0.010
	9	0.20	1.110	-1.609	0.104
	10	0.30	1.295	-1.204	0.258
	11	0.40	1.785	-0.916	0.579
	12	0.50	1.849	-0.693	0.615
	13	0.60	2.092	-0.511	0.738
	14	0.75	2.300	-0.288	0.833
Regime II.	15	0.90	2.190		
	16	1.20	2.232		
	17	1.50	2.054		

$[1]_0$	Fitted line	m	k_{obs} (h^{-1})
low (0.3 M)	y = 0.8894x + 0.3851	0.9	$k_{obs,1}$ = 1.47±0.27 h^{-1}
high (0.6 M)	y = 0.5424x + 0.9999	0.5	$k_{obs,2}$ = 2.72±0.49 h^{-1}

In the same way, the order of the electrophile (**1**) was determined in the non-saturated regime I, and the reaction rate dependence was found first-order in electrophile concentration. The data according to Fig. 6 in the article is presented on Table 4.
The order of the electrophile (**1**) was determined based on following equations:

$v = k_{obs}*[1]^n$
$\ln v = n*\ln[1] + \ln k_{obs}$

Table 4.: Reaction conditions and reaction rate using different β-nitrostyrene concentration

	Nr.	$[1]_0$ / M	v_0 / M*h^{-1}	ln $[1]_0$	ln v_0
$[2]_0$ = 0.3 M, catalyst: [3] = 0.006 M					
Non-saturated regime I.	1	0.30	0.480	-1.204	-0.734
	2	0.40	0.610	-0.916	-0.494
	3	0.50	0.860	-0.693	-0.151
	4	0.60	1.070	-0.511	0.068
	5	0.75	1.200	-0.288	0.182
Regime II.	6	0.90	1.160		
	7	1.00	1.101		
$[2]_0$ = 0.6 M, catalyst: [3] = 0.006 M					
Non-saturated regime I.	8	0.3	0.856	-1.204	-0.156
	9	0.4	1.339	-0.916	0.292
	10	0.5	1.668	-0.635	0.512
	11	0.7	2.092	-0.357	0.738
Regime II.	12	0.8	2.156		
	13	0.9	1.987		
	14	1.0	1.924		
	15	1.1	1.799		

$[2]_0$	Fitted line	n	k_{obs} (h^{-1})
low (0.3 M)	y = 1.0682x + 0.5458	1	$k_{obs,3}$ = 1.73± 0.31 h^{-1}
high (0.6 M)	y = 1.0292x + 1.1472	1	$k_{obs,4}$ = 3.15± 0.57 h^{-1}

In the same way, the order of the product (**4**) was determined.
In order to investigate the possible inhibition effect of the product, the reaction was monitored in the presence of different amount of the product (**R-4**) and different amount of enantiomer (**S-4**). The data according to Fig. 7 in the article is presented on Table 5. and the data according to enantiomer (**S-4**) is presented on Table 6.
The order of the product (**4**) was determined based on following equations:
$v = k_{obs}*[4]^p$
$\ln v = p*\ln[4] + \ln k_{obs}$

Table 5. Reaction conditions and reaction rate adding different amount R-product at the beginning of the reaction

Nr.	$[R\text{-}4]_0$ / M	v_0 / M*h^{-1}	ln $[R\text{-}4]_0$	ln v_0
1	0.1	0.899	-2.303	-0.107
2	0.2	0.757	-1.609	-0.278
3	0.3	0.480	-1.204	-0.735

Table 6. Reaction conditions and reaction rate adding different amount S-product at the beginning of the reaction

Nr.	$[S\text{-}4]_0$ / M	v_0 / M*h^{-1}	ln $[S\text{-}4]_0$	ln v_0
4	0.1	0.798	-2.303	-0.226
5	0.2	0.655	-1.609	-0.423
6	0.3	0.480	-1.204	-0.735

$[4]_0$	Fitted line	p	k_{obs} (h^{-1})
product (R)	y = -0.537x - 1.289	-0.5	$k_{obs,5}$ = 0.28±0.05 h^{-1}
enantiomer (S)	y = -0.454x - 1.218	-0.5	$k_{obs,6}$ = 0.30±0.05 h^{-1}

E. Calculation of activation energy

Activation energy was acquired by Arrhenius plot analysis. The reactions rates were determined at T = 274.15, 298.15 and 318.15 K. Reaction conditions: $[1]_0$ = 0.3 M, $[2]_0$ = 0.6 M; [3] = 0.006 M; solvent: $CHCl_3$. The data according to Fig. 9 in the article is presented on Table 7.

Table 7. Reaction rates at different temperature

T / K	(10^3/T) / (1/K)	v/ M*h^{-1}	ln (v/c_{cat}) / (s^{-1})
274.15	3.6476	0.486	-3.8
298.15	3.3540	1.122	-3.0
318.15	3.1432	1.700	-2.5

F. Calculation of association constant by NMR measurement using Job plot

The binding constants were evaluated by fitting the data to a 1:1 binding isotherm, and 1:1 binding was verified by Job plot. The binding constants were calculated from the changes in chemical shifts of catalysts protons. Nonlinear curve fitting was carried out with the Solver program in Excel. The binding constants K and the asymptotic change in chemical shift $\Delta\delta_{max}$ were chosen as the free parameters for fitting.

*Complex formation of catalyst (**4**) and acetylacetone (**2**)*

The complex of the nucleophile (acetylacetone, **2**) and the catalyst (**4**) was investigated. The catalyst concentration was varied between 0.02 and 0.2 M, while the concentration of the nucleophile was adjusted to get 0.2 M sum of concentration of each samples. The signals of catalyst were significantly shifted when adding the substrate. Signals of the

quinuclidine and some of the quinoline ring were changed. The most relevant peak belongs to the methoxy methylene of the catalyst (3H, δ_0 = 3.92 ppm, see on Figure 14.).

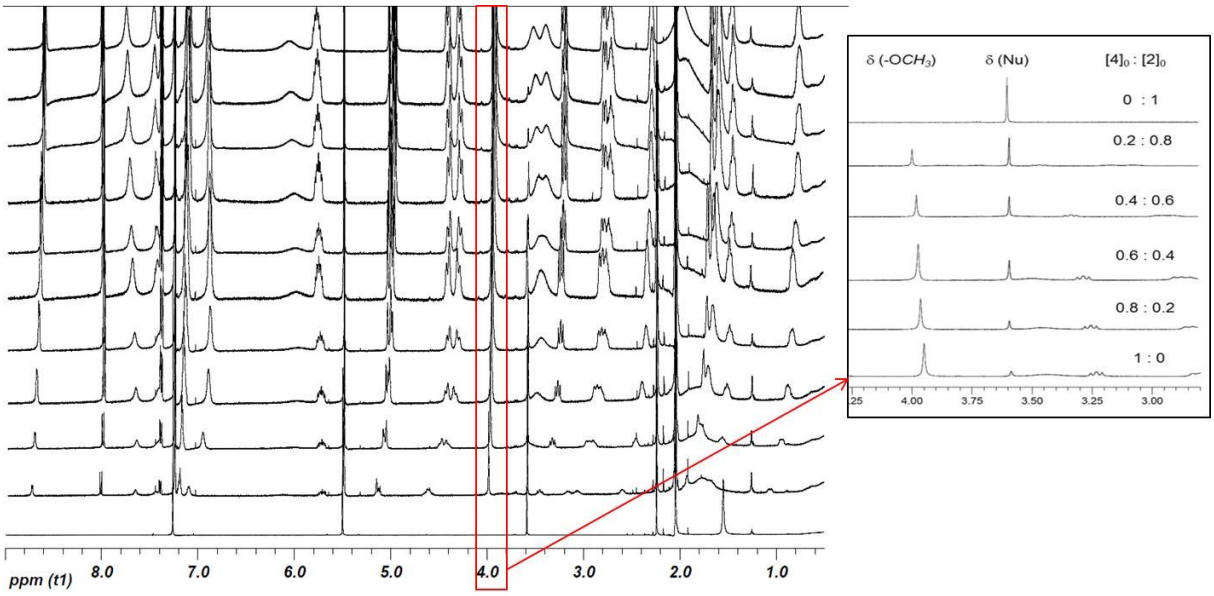

Figure 14. Chemical shifts of catalyst during Job-plot compared to free catalyst and the selected peaks for calculation of binding constant

*Job plot calculation for catalyst (**3**) - acetylacetone (**2**)complex formation*

Equations for determining binding constants:
$[Q]_0$ = initial concentration of catalyst **3**
$[A]_0$ = initial concentration of acetylacetone **2**
$[QA]$ = actual concentration of catalyst-acetylacetone complex

$$\delta_{obs} = X_Q\delta_0 + X_{QA}\delta_{max}$$

$$\delta_{obs} = \frac{[Q]_0 - [QA]}{[Q]_0}\delta_0 + \frac{[QA]}{[Q]_0}\delta_{max} = \delta_0 + \frac{[QA]}{[Q]_0}(\delta_{max} - \delta_0) = \delta_0 + \frac{[QA]}{[Q]_0}\Delta\delta_{max}$$

$$K_A = \frac{[QA]}{([Q]_0 - [QA])([A]_0 - [QA])}$$

$$([Q]_0 - [QA])([A]_0 - [QA]) = \frac{[QA]}{K_A}$$

$$[QA]^2 - \left([Q]_0 + [A]_0 + \frac{1}{K_a}\right)[QA] + [Q[_0[A]_0 = 0$$

$$[QA] = \frac{[Q]_0 + [A]_0 + \frac{1}{K_a} \pm \sqrt{([Q]_0 + [A]_0 + \frac{1}{K_a})^2 - 4[Q]_0[A]_0}}{2}$$

Table 8. Calculation of binding constant in Excel using Solver

$[Q]_0$ / M	X_Q	δ_{obs} (H-13)	$[QA]_{calc}$	δ_{calc}	$(\delta_{obs}-\delta_{calc})^2$ (res^2)	Sum res^2
0.020	1.0	3.924	0.0000	3.924		

0.018	0.9	3.932	0.0012	3.930	3.48E-06	
0.016	0.8	3.936	0.0023	3.937	5.35E-07	
0.014	0.7	3.941	0.0031	3.944	7.12E-06	
0.012	0.6	3.948	0.0036	3.951	7.46E-06	
0.010	0.5	3.956	0.0038	3.958	2.68E-06	
0.008	0.4	3.964	0.0036	3.964	3.57E-07	
0.006	0.3	3.972	0.0031	3.970	4.44E-06	
0.004	0.2	3.977	0.0023	3.975	4.31E-06	**3.039E-05**

$c_{total} = [Q]_0 + [A]_0 = 0.02\ M$

The calculated parameters: **K = 98.89±1.02 M^{-1}** and $\Delta\delta_{max}$ = **0.086±0.002 ppm**
Based on this parameters, the Job plot was determined:

Table 9. Calculation for Job plot

X_Q (Cat)	**X_A(Nu)**	**$\Delta\delta_{obs}$ (*H-13*)**	**$\Delta\delta$*X_Q**
1,0	0.0	0.000	0.0000
0.9	0.1	0.006	0.0055
0.8	0.2	0.013	0.0102
0.7	0.3	0.020	0.0138
0.6	0.4	0.027	0.0160
0.5	0.5	0.034	0.0168
0.4	0.6	0.040	0.0160
0.3	0.7	0.046	0.0138
0.2	0.8	0.051	0.0102
0.1	0.9	0.069	0.0069
0.0	1.0	0.000	0.0000